Available online at www.sciencedirect.com
ScienceDirect
Biochimica et Biophysica Acta 1763 (2006) 1284–1297
BIOCHIMICA ET BIOPHYSICA ACTA
BBA
www.elsevier.com/locate/bbamcr

Recognition of the tumor suppressor protein p53 and other protein targets by the calcium-binding protein S100B

Paul T. Wilder [a], Jing Lin [a], Catherine L. Bair [b], Thomas H. Charpentier [a], Dong Yang [a], Melissa Liriano [a], Kristen M. Varney [a], Andrew Lee, Amos B. Oppenheim [c], Sankar Adhya [b], France Carrier [a], David J. Weber [a,*]

[a] *Department of Biochemistry and Molecular Biology, The University of Maryland School of Medicine, 108 N. Greene St. Baltimore, MD 21201, USA*
[b] *National Institutes of Health, National Cancer Institute, 37 Convent Dr., Bethesda, MD 20892, USA*
[c] *Laboratory of Molecular Biology, Center for Cancer Research, NCI, National Institutes of Health, Bethesda, MD 20879, USA*

Received 15 July 2006; received in revised form 16 August 2006; accepted 17 August 2006
Available online 25 August 2006

Abstract

S100B is an EF-hand containing calcium-binding protein of the S100 protein family that exerts its biological effect by binding and affecting various target proteins. A consensus sequence for S100B target proteins was published as (K/R)(L/I)xWxxIL and matches a region in the actin capping protein CapZ (V.V. Ivanenkov, G.A. Jamieson, Jr., E. Gruenstein, R.V. Dimlich, Characterization of S-100b binding epitopes. Identification of a novel target, the actin capping protein, CapZ, J. Biol. Chem. 270 (1995) 14651–14658). Several additional S100B targets are known including p53, a nuclear Dbf2 related (NDR) kinase, the RAGE receptor, neuromodulin, protein kinase C, and others. Examining the binding sites of such targets and new protein sequence searches provided additional potential target proteins for S100B including Hdm2 and Hdm4, which were both found to bind S100B in a calcium-dependent manner. The interaction between S100B and the Hdm2 and/or the Hdm4 proteins may be important physiologically in light of evidence that like Hdm2, S100B also contributes to lowering protein levels of the tumor suppressor protein, p53. For the S100B–p53 interaction, it was found that phosphorylation of specific serine and/or threonine residues reduces the affinity of the S100B–p53 interaction by as much as an order of magnitude, and is important for protecting p53 from S100B-dependent down-regulation, a scenario that is similar to what is found for the Hdm2–p53 complex.

Keywords: S100B; Calcium-binding protein; S100 protein; p53; Hdm2; Mdm2

1. Introduction

There are several members of the S100 family of EF-hand Ca^{2+}-binding proteins that are distributed tissue-specifically in humans [1–3]. S100 proteins were given this name because they are *s*oluble in *100%* saturated ammonium sulfate [4]. One member, S100B, is a 21.5 kDa symmetric homodimer that is highly conserved (>97%) among mammals [1,4]. In general, low levels of S100B have trophic effects, and higher levels are problematic, resulting in uncontrolled cell growth [5–8]. Elevated levels of S100B are found in malignant melanoma [9–12], renal cell tumors [13] and malignant mature T-cells (such as doubly negative $CD4^-/CD8^-$ adult T-cells in leukemia patients) [14]. Furthermore, S100B is up-regulated by cytokines that stimulate gliosis such as interleukin-1β and the basic fibroblast growth factor [15]. As is the case for S100B, a number of other S100 proteins are regulated in a tissue-specific manner [16]. S100A1, S100A6 (calcyclin), and S100B are elevated significantly in metastatic human mammary epithelial cells [17], and increased levels of S100A4 in transgenic mice induce metastatic mammary tumors [18]. In the case of S100A4 (mts1), protein levels are controlled in benign cell lines via a *cis*-acting element 1300 base pairs upstream of the rat S100A4 start site [18], and expression of antisense RNA to S100A4 suppresses metastatic potential for a high-metastatic Lewis lung carcinoma [19]. Protein levels of S100B, S100A4, and S100A6 correlate with malignant melanoma, so these S100

* Corresponding author. Tel.: +1 410 706 4354; fax: +1 410 706 0458.
E-mail address: dweber@umaryland.edu (D.J. Weber).

0167-4889/$ - see front matter © 2006 Elsevier B.V. All rights reserved.
doi:10.1016/j.bbamcr.2006.08.024

proteins are used as markers for this cancer [20–23]. In general, S100 antibodies are used clinically to identify and classify cancer in several tissues and cell types including brain, bladder, breast, cervix, head and neck, intestine, kidney, larynx, lung, lymph, mouth, skin, and testes among others [13,14,17,24–38]. More recently, S100B was shown to not only be a prognostic marker, but that it also contributes to cancer progression in malignant melanoma by interacting with p53 and inhibiting its function as a tumor suppressor [24–26].

p53 is a transcription activator that signals for the up-regulation of genes involved in cell cycle arrest and apoptosis [27,28] and plays a pivotal role in the maintenance and regulation of normal cellular functions. Its inactivation affects cell cycle checkpoints, apoptosis, gene amplification, centrosome duplication and ploidy [28–35]. If p53 is mutated, as found in many human cancers, then the cell cycle proceeds unregulated, cell growth proliferates, apoptosis pathways are not induced, and proliferating cells transform into cancerous ones [29,36]. On the other hand, if p53 levels are too high, then phenotypes associated with aging and problems with skin and bone occur [37]. Thus, p53 is highly regulated by numerous post-translational modifications and via interactions with other proteins (i.e. S100B, Hdm2, etc.) to regulate its activity [31,38–41].

In its most active form, p53 is a dimer of dimers to form a tetrameric X-type four-helix bundle in its C-terminus [42–44]. Upon binding specific DNA promoter sequences, the p53 tumor suppressor activates the transcription of numerous downstream target genes including a cyclin-dependent kinase inhibitor ($p21^{WAF/CIP1}$), cell cycle control proteins (cyclin G, GADD45), genes involved in apoptosis (i.e. Bax), and a gene product, Mdm2 (or Hdm2 for the human protein), which in turn negatively regulates p53 protein levels inside the cell as part of a feedback loop to keep p53 protein levels in check [27,28,45]. Hdm2 is an E3 ligase that down-regulates p53 by an ubiquitin-mediated pathway, which is dependent on the phosphorylation state of p53 in the N-terminal transactivation domain. The 3D structure of the N-terminal domain of Hdm2 somewhat resembles EF-hand proteins, despite the fact that it does not bind calcium [46]. A structurally related protein, Hdm4 (also called Mdmx or Mdm4 for the murine protein) also binds to the same region of p53 and inhibits its activity under certain conditions; however, unlike Hdm2, Hdm4 does not have significant ubiquitin ligase activity [47]. Directly C-terminal to the tetramer domain on p53 is a basic region termed the "extreme C-terminus" or the "C-terminal negative regulatory domain", which is unstructured when free in solution, but is helical when bound to the calcium-binding protein S100B [48]. If the negative regulatory domain is unmodified, p53 has lowered transcription activation activity (i.e. latent state). In fact, deletion of the last 30 residues, covalent modification, and/or binding of antibodies to this domain activates p53 by preventing non-specific DNA binding and/or perhaps by inhibiting S100B binding [49,50]. In this study, it is demonstrated that phosphorylation of the C-terminus does indeed inhibit S100B binding and is analogous to how p53 is protected from another known negative regulator of p53, namely Hdm2. Furthermore, it is shown that S100B interacts directly with Hdm2 in a calcium-dependent manner. Thus, it is possible that S100B and Hdm2 work concertedly to down-regulate p53, which is discussed.

2. Materials and methods

2.1. Chemicals

All chemicals and reagents were ACS grade or higher and purchased from Sigma-Aldrich unless otherwise indicated. $^{15}NH_4Cl$ was purchased from Cambridge Isotope Laboratories (Woburn, MA). All buffers were passed through Chelex-100 resin to remove trace metals.

2.2. Peptides and S100B protein preparation

Unlabeled and ^{15}N-labeled S100B were overexpressed and purified from *E. coli* as described previously [51,52]. Using phage display, Ivanenkov et al. defined a target sequence ([K/R]-[L/I]-x-W-x-x-I-L) and identified a 12 residue peptide, termed TRTK-12, which binds S100B and most closely resembles a sequence (residues 265–276) in the actin capping protein, CapZ (62). By expanding protein database searches to include a larger number of protein sequences ([K/R]-[L/I]-[P/S/N/D]-[W/L/I]-[S/D/L]-x-[L/I]-[L/F]), additional S100B targets were identified (Table 1). Peptides based on such searches were produced by Bio-Synthesis, Inc. (Lewisville, Texas) using solid-state peptide synthesis and their purity were >95% as determined by HPLC and mass spectrometry unless indicated otherwise (see Table 1 for the amino acid sequences). The concentration of peptides containing tryptophan were determined using the extinction coefficient for tryptophan ($\varepsilon_{280}=5690\ cm^{-1}\ M^{-1}$), the concentration of the FITC labeled p53 peptide, FITC-$p53^{367-393}$ was determined using the extinction coefficient for FITC ($\varepsilon_{494}=72{,}000\ cm^{-1}\ M^{-1}$), while the concentration and composition of the other peptides were confirmed by amino acid analysis (Bio-Synthesis, Inc., Lewisville, Texas). The N- and C-termini were acetylated and amidated, respectively, for TRTK-12 (Biopolymer Lab, U. of Maryland, Baltimore, MD), $^{F385W}p53^{367-388}$, RAGE, $p53^{367-388}$, $p53^{321-346}$, $Hdm2^{25-43}$, $Hdm4^{25-43}$, and $PAK1^{252-271}$ peptides. The N-terminus of $p53^{367-393}$ was acetylated as were the N-terminus of the phosphorylated serine/threonine version of that peptide, S376 Phos ($p53^{367-393}$ phosphorylated at Ser-376), T377 Phos ($p53^{367-393}$ phosphorylated at Thr-377), S378 Phos ($p53^{367-393}$ phosphorylated at Ser-378), S392 Phos ($p53^{367-393}$ phosphorylated at Ser-392), and acetylated lysine version of $p53^{367-393}$, K382 Ac ($p53^{367-393}$ acetylated at Lys-382), while for the FITC-p53 peptide, the N-terminus only of $p53^{367-393}$ is conjugated to FITC. The C-terminus of RKLLW (Alexis Biochemical, San Diego, CA) was amidated. The termini of Nt, an Y11W mutant of neurotensin (residues 8–13; American Peptide, Sunnyvale, CA), XP-1, the xenopsin related peptide 1 (Bachem Inc.), PKC^{19-36} (Sigma-Aldrich), and PKC A25S (Sigma-Aldrich) were not modified at either the N- or the C-termini.

2.3. Fluorescence spectroscopy

The Ca^{2+}-dependent interaction of peptides with wild-type and mutants of S100B were performed using fluorescence spectroscopy techniques on an SLM-Aminco Bowman series 2 (Thermo, Asheville, NC) or a Carey Eclipse (Varian Inc., Palo Alto, CA) fluorescence spectrophotometer with the temperature maintained at 37 °C. For low salt conditions listed in Table 1, the buffer contained 10 mM TES, pH 7.2, 15 mM NaCl, and 10 mM $CaCl_2$; the high salt buffer contained 100 mM KCl in addition to that listed in the "low salt" buffer. For the Trp containing peptides ($^{F385W}p53^{367-388}$, TRTK-12, RAGE, RKLLW, XP-1, and Nt), increased fluorescence emission from the tryptophan residue at 338 nm was monitored upon titration of S100B with excitation at 295 nm. In all of the titrations, the titrant and reactant were prepared with equal concentrations of peptide (up to 4 mM), so no corrections for dilution were necessary. Fluorescent polarization measurements during competition binding studies was used to monitor the binding of peptides to S100B using the same low and high salt conditions except with 1 μM FITC-$p53^{367-393}$. Polarization readings of FITC-$p53^{367-393}$ were monitored is such assays using an SLM-Aminco series 2

Table 1
Summary of S100B binding peptides[a]

	~K_D (μM)		Reference
Binding in low salt (15-30 mM)[b]			
F385W p53 (367–388)	3.9±0.27	SHLKSKKGQSTSRHKKLMWKTE	[69]
TRTK-12[c]	7.0±0.43	TRTKIDWNKILS	[88,89]
RAGE (42–59)	11.7±0.02	PKKPPQRLEWKLNTGRTE	New Data
Ndr (62–87)	20.0±10.0	KRLRRSAHARKETEFLRLKRTRLGLF	[63]
p53 (367–393)	22.5±6.80	SHLKSKKGQSTSRHKKLMFKTEGPDSD	New Data
p53 (367-388)	23.5±6.60	SHLKSKKGQSTSRHKLMFKTE	[69]
RKLLW	35.0±2.15	RKLLW	New Data
XP-1	44.1±1.80	HPKRPWIL	New Data
Neurotensin Y11W (8-13)	53.4±0.44	RRPWIL	New Data
High salt (125-130 mM)			
Hdm4 (25-43)[d]	0.4±0.02	NQVRPKLPLLKILHAAGAQ	New Data
Hdm2 (25-43)[d]	3.1±0.35	ETLVRPKPLLLKLLKSVGA	New Data
TRTK-12[c]	17.2±2.31	TRTKIDWNKILS	[88,89]
F385W p53 (367-388)[d]	17.3±2.54	SHLKSKKGQSTSRHKKLMWKTE	New Data
p53 (367-393)[d]	99.2±7.71	SHLKSKKGQSTSRHKKLMFKTEGPDSD	New Data
p53 (325-355)[e]	112.0±7.00	GEYFTLQIRGRERFEMFRELNEALELKDAQA	[90]
p53 (325-339)[e]	172.0±4.00	GEYFYLQIRGRERFE	[90]
p53 (340-351)[e]	302.0±7.00	MFRELNEALELK	[90]
p53 (305-322)[e]	NB	KRALPNNTSSSPQPKKKP	[90]
p53 (293-393)[e,f] Site 1	0.25±0.05	GEYFTLQIRGRERFEMFRELNEALELKDAQA	[90]
Site 2	16.0±2.00	SHLKSKKGQSTSRHKKLMFKTEGPDSD	
Modified p53(367-393)[g]			
S376 Phos	239.9±6.80	SHLKSKKGQ*S*TSRHKKLMFKTEGPDSD	New Data
T377 Phos	92.7±44.0	SHLKSKKGQS*T*SRHKKLMFKTEGPDSD	New Data
S378 Phos	41.3±14.2	SHLKSKKGQST*S*RHKKLMFKTEGPDSD	New Data
S392 Phos	41.5±5.60	SHLKSKKGQSTSRHKKLMFKTEGPD*S*D	New Data
K382 Ac	218.3±21.9	SHLKSKKGQSTSRHKKLMFKTEGPDSD	New Data
Other peptides			
PKC (19-36)[h]	ND	RFARKGALRQRNVHQVKN	New Data
p53 (321-346)[h]	ND	YFTLQIRGRERFEMFRELNEALELKD	New Data
ROS-GC1 (962-981)[i]	0.198+0.11	CYRIHVNRSTVQILSALNEGF	[91]
p53 (319-393)[j]	0.025+0.01	GEYFTLQIRGRERFEMFRELNEALELKDAQA	[92]
Mu p53(321-346)[j]	ND	WWTLQIRGRERFEMFRELNEALELKD	[92]
Mu p53 (357-381)[j]	ND	RAHSSYLKTKKGQSTSRHKKTMVKK	[92]
PKCA25S (19-36)[k]	ND	RFARKGSLRQRNVHQVKN	[93]
Nm (37-53)[k]	ND	KIQASFRGHITRKKLKG	[93]
MARCKS (152-172)[l]	ND	SFKKSFKLSGFSFKKNKKEAG	[94]
Tau (337-370)[m]	ND	VEVKSEKLDFKDRVQSKIGSLDNI	[95]
Melittin[m]	ND	GIGAVLKVLTTGLPALISWIKRKRQQ	[95]

fluorescence spectrophotometer at 37 °C with an excitation wavelength of 85 nm and an emission wavelength of 520 nm. The binding data were fit using a single site binding model with Origin software (OriginLab Corp., Northampton, MA) and one peptide bound per S100B subunit. For fluorescent intensity competition assays with the ^{F385W}p53$^{367–388}$ peptide, non-fluorescent peptide was used to compete ^{F385W}p53$^{367–388}$ with the upper limit for the dissociation constant (K_D) being determined using the Cheng–Prusoff equation; $K_D=[I]_{50}/(1+[F385W]/{}^{F385W}K_D)$ where $[I]_{50}$ is the concentration of the unlabeled peptide at 50% inhibition and $^{F385W}K_D$ is the dissociation constant of the S100B-^{F385W}p53$^{367–388}$ complex (in low salt $^{F385W}K_D=3.9\pm0.3$ μM; Table 1) [53]. For fluorescence polarization competition assays, an equation derived by Nikolovska-Coleska et al. was used for determination of the K_D, as previously described [54], using; $K_D=[I]_{50}/([L]_{50}/{}^{FITCp53}K_D+[P]_0/{}^{FITCp53}K_D+1)$ where $[I]_{50}$ is the concentration of the unlabeled peptide at 50% inhibition, $[L]_{50}$ is the concentration of the free FITC-p53 at 50% inhibition, $[P]_0$ is the concentration of the free protein at 0% inhibition, and $^{FITCp53}K_D$ is the dissociation constant of the S100B-FITC p53$^{367–393}$ complex (in high salt $^{FITCp53}K_D=99.2\pm7.7$ μM; Table 1) [54].

2.4. Isothermal titration calorimetry (ITC)

Heat changes during the titration of the Hdm2$^{25–43}$, Hdm4$^{25–43}$, PAK1$^{252–271}$, and ^{F383W}p53$^{367–388}$ peptides into Ca^{2+}-S100B was measured using a VP-ITC titration microcalorimeter (MicroCal, Inc., Northhampton, MA) as done previously [55]. For each titration the sample cell (1.4 ml) contained 10 mM TES, pH 7.2, 15 mM NaCl, and 10 mM $CaCl_2$, 100 mM KCl, and 0.1 mM S100B while the reference cell contained water with all solutions being degassed under vacuum and equilibrated at 37 °C prior to titration. Upon equilibration, a 1.25–1.8 mM peptide solution prepared in the same buffer without S100B was injected in 29×5 μL aliquots using the default injection rate with a 300 s interval between each injection to allow the sample to return to baseline. The resulting titration curves were corrected for the protein free buffer control and analyzed using the Origin for ITC software supplied by MicroCal (Northampton, MA).

2.5. NMR spectroscopy

NMR spectra were collected at 37 °C with either a Bruker DMX600 NMR spectrometer (600.13 MHz for protons) or a Bruker AVANCE 800 NMR spectrometer (800.27 MHz for protons) equipped with four frequency channels and a triple-resonance z-axis gradient 5 mM cryoprobe. All proton chemical shifts are reported with respect to the H_2O or HDO signal taken to be 4.658 ppm relative to external TSP (0.0 ppm) at 37 °C. The ^{15}N chemical shifts were indirectly referenced using the following ratios of the zero-point frequencies at 37 °C: 0.10132905 for ^{15}N [56–58]. Uniformly ^{15}N-labeled S100B was used to collect the 2D ^{1}H,^{15}N-fast HSQC [59] during the titration of peptides into Ca^{2+}-S100B and changes in S100B backbone ^{15}N and ^{1}H were monitored and readily assigned. Typical NMR samples contained 0.05–0.50 mM S100B, 0–5.0 mM peptide, 10 mM TES, pH 7.2, 15 mM NaCl, 10 mM $CaCl_2$, 0.34 mM NaN_3, 5–10% D_2O.

2.6. Lambda2Hybrid protein association assay

Under normal conditions, double infections of *E. coli* by lambda phage do not occur; however, expressing protein binding partners fused to the C-terminus of phage D protein enables the two phages to associate and simultaneously infect a cell. By using modified lambda phage, which contains different antibiotic resistances, the interaction and formation of multi-lysogens will result in double antibiotic resistant colonies (Cm^r/Kan^r). Such colonies can then be quantified as the formation of specific protein–protein complexes; furthermore, disruption of such protein–protein interactions are also performed in inhibition assays since the interaction between the two phages is done in vitro. Construction of the S100B (λD-S100B$_C$), wild type human p53 (λD-p53$_K$), dimeric p53 mutant (λD-p53$_K^{MLQR}$) [60] and Hdm2 (λD-Hdm2$_K$) display phages were done according to the method of Bair, et al. (in preparation). For the association assay, the phage fusions being tested are first diluted separately then combined at a ratio of 1:1 in the reaction tube, mixed gently and incubated for 5 min at R/T. To this, 100 μL SABE buffer (20 mM Tris, pH 7.4, 10 mM $CaCl_2$, 10 mM $MgSO_4$, 100 mM NaCl, and 5 mM EDTA) with or without inhibitor is added with gentle mixing and incubated for 10 min at room temperature. At that time, 1×10^8 mid-log phase *E. coli* C600

Notes to Table 1:

[a] The underlined amino acids are within 6 Å of residues in S100B based on the observance of NOE correlations for determining the NMR based structures of p53$^{367–388}$ [86], TRTK [88], and Ndr [63] peptides bound to Ca^{2+}–S100B. The short hand notation NB was used to indicate "No binding" to the peptide was observed, and ND was used to indicate that the peptide binds to S100B but that the exact K_D is "not determined".

[b] Binding affinities in "low salt" conditions were performed by fluorescence spectroscopy or with isothermal titration calorimetry (ITC; for TRTK-12) with in 15 mM TES, pH 7.2, 10 mM $CaCl_2$, 15 mM NaCl, at 37 °C except for Ndr that was determined by Bhattacharya et al. by plotting the chemical shift changes determined by NMR in 20 mM Tris, pH 7.5, 5 mM $CaCl_2$, 30 mM KCl, and 10 mM DTT at 37 °C [63].

[c] The TRTK-12 peptide is derived from residue 265 to 276 of the actin capping protein CapZ peptide, which was discovered by Dimlich et al. [62]. Previously, McClintock et al. report that TRTK-12 binds S100B with a $K_D=0.27\pm0.03$ μM in 50 mM Tris, 50 mM KCl, and 1 mM $CaCl_2$ at pH 7.2 [65,88,89].

[d] The buffer conditions were 10 mM TES, pH 7.2, 10 mM $CaCl_2$, 15 mM NaCl, 100 mM KCl, at 37 °C.

[e] Fernandez-Fernandez et al. [90] reported binding for p53$^{325–355}$, p53$^{325–339}$, p53$^{340–351}$, p53$^{305–322}$, and p53$^{293–393}$ in 25 mM Tris, pH 7.5, 10 mM $CaCl_2$, 99.2 mM NaCl, 1 mM DTT. This group also determined the binding affinity for p53$^{367–393}$ under these conditions, which gave the same affinity for Ca^{2+}–S100B ($K_D=102\pm3$ μM) as reported here for the "high salt" buffer.

[f] The domain encompassing the tetramerization and C-terminal regulatory region of p53 was synthesized and two S100B binding sites were detected; these are likely the tetramerization site (residues 325 to 355) and in the C-terminal regulatory region (residues 367 to 393) [90].

[g] The p53$^{367–393}$ peptide was covalently modified in the C-terminal region of p53 to mimic covalent modifications that occur in vivo such as phosphorylation (Phos) and acetylation (Ac), which are italicized.

[h] NMR experiments show the PKC$^{19–36}$ and p53$^{321–346}$ bind S100B in 10 mM TES, pH 7.2, 10 mM $CaCl_2$, 15 mM NaCl, at 37 °C, but the exact K_D was not determined.

[i] A peptide from rod outer segment membrane guanylate cyclase type 1 (ROS-GC1; residues 962 to 981) was immobilized to a sensor chip via the cysteine thiol group, from a Cys residue added to the N-terminal of the peptide, and surface plasmon resonance (SPR) was used to determine the binding affinity [91].

[j] The C-terminal domain of human p53 (residues 319–393) was immobilized to a sensor chip by random coupling of its amine groups and SPR was used to determine the binding affinity to S100B [92]. Subsequently, two shorter peptides derived from mouse p53, Mu p53$^{321–346}$ and Mu p53$^{357–381}$, were added to compete off S100B; the K_D for this competition was not reported (ND). While the tetramerization domain peptide, Mu p53$^{321–346}$, was able to compete off S100B the C-terminal peptide, Mu p53 $^{357–381}$, was not able displace S100B at concentrations as high as 1 μM. Note that the sequence of the mouse p53 peptide, Mu p53$^{357–381}$, differs from the human p53 peptide, p53$^{367–388}$ at three positions (L383M, residue colored in gray; R379H, F385K; human numbering), which are important for binding S100B. The Mu p53$^{321–346}$ peptide was mutated at two positions (Y321W, F322W; human numbering).

[k] S100B inhibits the PKCα phosphorylation of these peptides as it does the p53$^{367–388}$ peptide by binding the peptide [93].

[l] The MARCKS peptide (residues 152 to 172) contain a PKCα phosphorylation site whose phosphorylation is inhibited due to binding to S100B but the affinity is undetermined [94].

[m] Baudier et al. showed the interaction of Tau peptide (residues 337 to 370) with S100B and the Tau$^{337–370}$ peptide contains a PKCα phosphorylation site. In addition, these authors also report that Melittin, a 26 amino acid long peptide from bee venom, also binds S100B, but for both of these peptides, no K_D is reported [95].

(*sup*E$^+$) cells are grown in LB supplemented with 0.4% maltose and 10 mM $CaCl_2$. After 45–60 min at room temperature, the entire reaction is plated on one 100 mm LB agar plate containing 12 μg/ml chloramphenicol and 25 μg/ml kanamycin and incubated overnight at 32 °C, after which time, the number of colonies are counted.

2.7. GST-Hdm2 pull down assay

The GST-Hdm2 expression vector was prepared in the laboratory of Allan M. Weissman (NCI, NIH, Bethesda, MD 20892) and provided by Shengyun Fang (The University of Maryland School of Medicine, Baltimore, MD). This vector was used to produce glutathione S-transferase (GST) fusions of Hdm2 with a N-terminal GST tag in *E. coli* BL-21(DE3)star cells (Novagen Inc.) that were grown at 37 °C until mid-log phase (i.e. OD_{600} ~ 0.8–1.0), induced with 0.84 mM IPTG for 1–1.5 h after which the cells were centrifuged 5000×*g* in a GS-3 rotor using a RC2-B Superspeed centrifuge (Thermo, Asheville, NC) and the pellet stored at −80 °C until use. Bacterial pellets were suspended in 1 ml per gram with 50 mM Tris, pH 7.4, 150 mM NaCl, 5 mM DTT, 2 mM phenylmethylsulfonyl fluoride (PMSF) to which 0.08 ml per gram pellet of 10 mg/ml lysozyme was added for 15 min on ice. Then, 300 μl DNase solution (1 mg/ml) and 300 μl 4.9 M $MgCl_2$ were mixed for 15 min and lysis was completed by probe sonication. The sonicate was clarified by centrifugation at 4 °C for 45 min at 27,000×*g* in SS-34 rotor (Sorvall), the protein was captured on glutathione agarose beads (Novagen) using batch purification, and the beads were washed three times in 50 mM Tris, pH 7.4, 150 mM NaCl. GST-Hdm2 beads and control beads were then blocked with 5% BSA in the same buffer for 30 min at 37 °C, centrifuged briefly to pellet beads then washed with the same buffer without BSA with either 5 mM $CaCl_2$, no $CaCl_2$, or no $CaCl_2$ plus 5 mM EDTA and pelleted again before adding 10 μg S100B in the same buffer for 1 h at room temperature. The beads were then washed three times in the same buffer, without S100B, to remove unbound protein before the S100B was eluted with 25 μl EDTA (500 mM). Samples were run on an 18% SDS-PAGE, blotted, and detected using S100B rabbit polyclonal antibody (Research Diagnostics Inc., Flanders, NJ) at 1:1000 dilution as done for the cellular p53 assays outlined below.

2.8. Cellular assays of p53 down-regulation by S100B

Human large cell lung carcinoma cells, H1299, were grown in Minimum Essential Medium (Invitrogen Inc.) containing 10% fetal bovine serum. The p53 expression vector (pCMV3-p53) was provided by Bert Vogelstein (Johns Hopkins University, Baltimore, MD). Using this wild-type p53 expression vector and the QuikChange site-directed mutagenesis kit (Stratagene Inc.), the phosphorylation site single and double mutant constructs were engineered including pCMV3.p53 S376A(TCT to GCC), pCMV3.p53 T377A (ACC to GCC) and pCMV3.p53 DM (S376A T377A). The pCMV3 empty vector, which was used as a control in several experiments, was purchased (Strategene Inc.). The pCMV-Myc empty vector was purchased (Clontech Inc.), and the gene for rat S100B was cloned into the *Sal*I/*Xho*I sites. To examine the effects that S100B has on p53 protein levels and function, H1299 cells were transiently transfected with the fixed amount of plasmid (12 μg) by the Fugene 6 transfection reagent (Roche Diagnostics) according to the manufacturer's recommendation such that the S100B plasmid was in excess (9 μg) versus the p53 plasmid (3 μg). Next, western blot analyses were performed on 20 μg of H1299 protein extract after the cells were lysed in RIPA buffer (50 mM Tris–HCl, pH 7.5, 150 mM NaCl, 1% Nonidet P-40, 0.5% sodium deoxycholate, 0.1% SDS, 1 mM phenylmethylsulfonyl fluoride, 2 μg/ml leupeptin, 5 mM DTT, 50 mM NaF, 5 mM EDTA). The proteins were analyzed on a 12% polyacrylamide gel, transferred on nitrocellulose, and reacted with either p53 mouse monoclonal antibody (DO-1, Oncogene Research Products, Boston, MA) at 1:1000 dilution, S100B rabbit polyclonal antibody (Research Diagnostics Inc., Flanders, NJ) at 1:1000 dilution, p21 rabbit monoclonal antibody (Zymed Laboratories Inc.) at 1:1000, or actin mouse monoclonal antibody (Oncogene Research Products) at 1:5000 dilution to control for even protein loading. The blots were then reacted with their respective secondary antibodies conjugated to horseradish peroxidase and reacted with a chemiluminescence substrate (ECL, GE Healthcare) as recommended by the manufacturer.

3. Results

3.1. Binding of S100B to peptide and protein targets including p53, Hdm2, and Hdm4

Upon the addition of calcium, helix 3 of S100B rotates ~90° and exposes a site that binds target proteins and peptides [61]. Using phage display, Ivanenkov et al. defined a S100B target

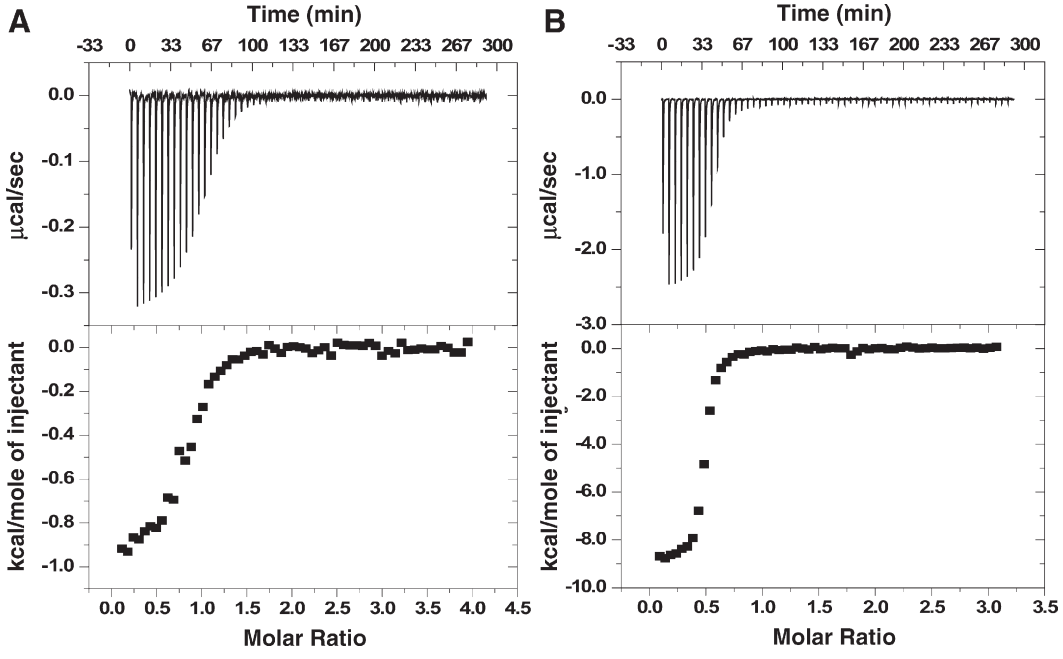

Fig. 1. Thermodynamic binding data showing that peptides derived from Hdm2 residues 25 to 43 ($Hdm2^{25–43}$) and Hdm4 residues 25 to 43 ($Hdm4^{25–43}$) bind S100B in the presence of calcium. Isothermal titration calorimetry (ITC) data demonstrating the calcium-dependent interaction between (A) S100B and $Hdm2^{25–43}$, and (B) S100B and $Hdm4^{25–43}$ in 10 mM TES, pH 7.2, 15 mM NaCl, and 10 mM $CaCl_2$, 100 mM KCl, and 0.1 mM S100B at 37 °C.

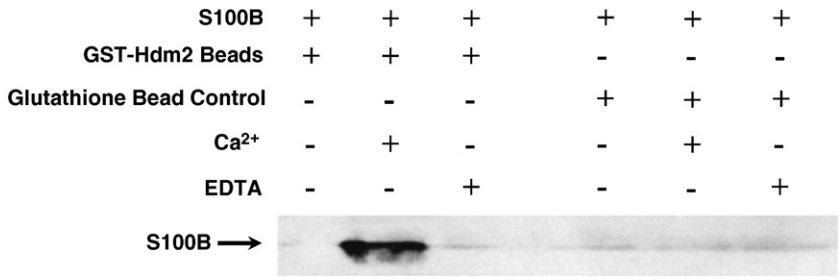

Fig. 2. GST-Hdm2 pull down assay showing the Ca^{2+}-dependent interaction between S100B and Hdm2. An N-terminal GST tagged Hdm2 was immobilized on glutathione beads and S100B (±EDTA) or Ca^{2+}-S100B was loaded and washed extensively with buffer (without S100B). A subsequent wash with EDTA was used to release any S100B bound to the Hdm2-linked column. Only in the presence of Ca^{2+} is S100B able to bind immobilized GST-Hdm2 (lane 2). No binding was observed without calcium present (lane 1) or in controls with EDTA in the loading buffer (lanes 3, 6), GST-bound beads (4, 5, 6) or with beads alone (data not shown).

sequence ([K/R]-[L/I]-x-W-x-x-I-L) and identified a 12 residue peptide, termed TRTK-12, which binds S100B and most closely resembles a sequence (residues 265–276) in the actin capping protein, CapZ [62] (Table 1). By expanding the search to include a larger number of protein sequences ([K/R]-[L/I]-[P/S/N/D]-[W/L/I]-[S/D/L]-x-[L/I]-[L/F]), additional S100B targets were identified. Of particular interest was the discovery that S100B associates rather tightly to peptides derived from Hdm2 (K_D=3.1±0.4 μM; Fig. 1A; Table 1) and Hdm4 (also termed MdmX; K_D=0.4±0.02 μM; Fig. 1B, Table 1) since these two proteins are involved in the regulation of p53. In addition to these two peptides, several other peptides were also found to bind S100B in the presence of calcium including new data reported here for peptides derived from p53, phosphorylated p53, human RAGE, neurotensin (nt), cathepsin L inhibitor (RKLLW), and a peptide derived from the regulatory domain of protein kinase Cα (0.3 μM<K_D<60 μM; Table 1). That Hdm2 does indeed bind S100B in a calcium-dependent manner was further supported by GST-pull down experiments using full-length S100B and Hdm2 protein constructs (Fig. 2). It should be pointed out that the Hdm2 peptide, which binds S100B (Table 1), is derived from a region of the protein that is not exposed in existing X-ray or NMR structures (PDB codes 1Z1M, 1T4F, 2AXI, and 1RV1). Therefore, the interaction observed between S100B and full-length Hdm2 (Fig. 2) must either occur as the result of exposing this Hdm2 peptide site upon binding or alternatively S100B interacts with yet another region of Hdm2.

Upon examination of Table 1 and NMR solution structures of S100B–peptide complexes [48,63–65], there is not a very well defined consensus sequence for S100B targets, which may be the reason why S100B is able to bind such a diverse class of proteins. The one common element in all of the S100B–peptide structures completed to date (TRTK-, $p53^{367–388}$-, and Ndr-S100B) and in all of the sequences of the S100B target peptides is that there is a hydrophobic residue on the target peptide (W, F, or L residues) that interacts with several hydrophobic residues on helices 3 and 4 of S100B (highlighted in gray in Table 1). A second component of a S100B target protein is the presence of several positively charged Lys and Arg residues on either side of the hydrophobic residue. Such basic residues likely form salt bridge(s) with acidic residues on S100B; however, there is a great deal of variation in the position of basic residues in the peptides' sequences (colored blue in Table 1). For example, ionic interactions in the S100B–p53 structure (i.e. between Glu-45 and Glu-86 of S100B and Arg-379 and Lys-386 on p53, respectively) are observed in this 3D structure and are further supported by the observation that $p53^{367–388}$ binds Ca^{2+}–S100B nearly 5-fold weaker at elevated salt concentrations; similarly, TRTK-12, which also has potential salt bridges binds S100B 2.5-fold weaker at higher salt. The lesser effect on TRTK-12 is likely due to the extensive number of hydrophobic interactions observed in the structure of this peptide bound to S100B (Table 1) [48,64]. Although not yet supported by 3-dimensional structural data, it appears that the presence of positively charged arginine and lysine flanking both sides of the hydrophobic residue may tighten the interaction since the peptides that only have a positive charges on one side (i.e. RKLLW, XP-1, and Nt) bind more weakly; however, it should also be noted that these peptides are shorter as well, so the decreased affinity could also be due to lack of another interaction(s).

3.2. Chemical shift perturbations in S100B caused by target peptide binding

To further explore interaction of S100B with various target peptides, changes in the chemical shifts of S100B backbone ^1H and ^{15}N between Ca^{2+}-bound to target peptide–Ca^{2+}-bound were recorded (Fig. 3). The amino acids in S100B where chemical shift values are perturbed upon binding of different target peptides are very similar indicating that the target peptides as a whole interact with similar residues on S100B (Fig. 3); although, it should be noted that chemical shift changes in a protein may be the result of direct interaction of a ligand with amino acid residues and/or by changes in the overall protein structure caused by peptide binding. For the five S100B–peptide interactions examined here (Fig. 3), significant chemical shift perturbations and/or residues that are exchange broadened (i.e. resonances that disappear in peptide titrations) occur for residues in loop 2, termed the hinge region (S41, F43, L44, E45), helix 3 (V52, V53, V56, T59), the C-terminus of helix 4 (S78–F88), and in helix 1 (F14). With Phe-14 as an exception[1], most of these

[1] Resonances of phenylalanine-14 in S100B likely shift during the titrations with the peptides because of a long-range structural perturbation rather than from a direct interaction with the S100B-binding peptides.

residues that show chemical shift perturbations in the five peptide complexes are also found to interact directly in the S100B–p53 peptide complex (via intermolecular NOE correlations) including residues in the hinge region of S100B (L40, H42, L44, I47), helix 3 (V52, V56), and in C-terminus of helix 4 (M79, V80, A83, F87) [48]. Interestingly, when the amino acid

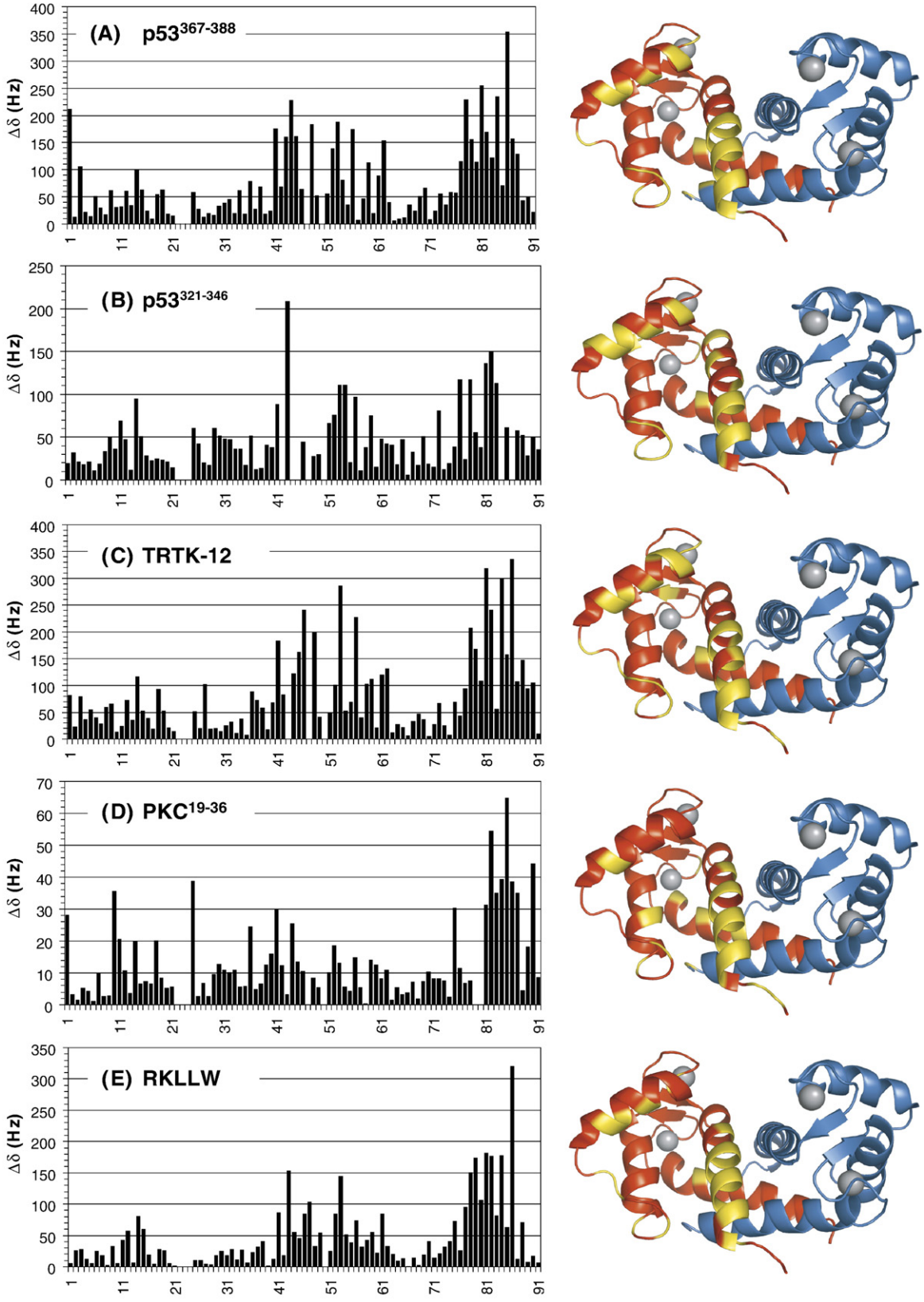

sequences of human S100 proteins are compared (Fig. 4), the hydrophobic nature of the residues in S100B that interact with the target peptides are conserved throughout the family of 22 related S100 proteins including L40 (95.0%), L44 (85.0%), V52 (75.0%), V53 (100.0%), V56 (90.0%), V80 (100.0%), A83 (75.0%), F87 (60.0%) and F88 (65.0%). However, the negatively charged residues that interact with specific peptide targets are not well conserved. For example, the charged residues of S100B that interact with $p53^{367–388}$ are minimally conserved including E45 (15.0%) and E46 (25.0%) or E86 (50.0%), and in some cases, other S100 proteins have these analogous positions (i.e. E45, E46, and E86 in S100B) replaced with oppositely charged Lys or Arg residues, 35.0%, 15.0%, and 30.0% of the time, respectively. It is these variations in the charged residues that could perhaps give rise to binding specificity among various S100 proteins.

3.3. Do full-length Hdm2 and p53 interact with the well-defined peptide binding site on S100B?

Data in Table 1 and several previously published studies have demonstrated that S100B interacts with p53 including full-length p53 [66] and peptides derived from the C-terminal region of p53 [48,67–69]. However, the binding site for full-length p53 on S100B has not yet been fully established. Nor has it been established whether Hdm2 binds to this same site on Ca^{2+}-bound S100B or to another yet to be discovered site. To answer this question, a newly developed method for examining protein–protein interactions was employed, which was developed by Dr. Sankar Adhya and colleagues at the National Cancer Institute, and termed the Lambda-2-hybrid method.

Specifically, competitive inhibition experiments using the Lambda-2-hybrid methodology (Bair et al., in preparation) confirmed that full-length p53 binds to a site on S100B that overlaps a small molecule inhibitor binding site (SBi1) and the TRTK-12 peptide site on S100B. In both of these experiments, recombinant lambda phage expressing S100B (λD-S100B) interacts with lambda phage expressing p53 (λD-p53) or a dimeric mutant of p53 (λD-$p53^{MLQR}$; [60]) each of which are fused to the C-terminus of the phage major capsid protein D. Importantly, the S100B–p53 interactions detected by this method could be inhibited specifically by either the TRTK-12 peptide or by the S100B small molecule inhibitor, SBi1 (Fig 5). Similarly, a lambda phage expressing Hdm2 (λD-Hdm2) interacts with λD-S100B and this Hdm2-S100B protein–protein interaction was also inhibited by TRTK-12. It was also demonstrated that Hdm2 display phage, λD-$Hdm2_k$, does interact with the λD-p53 and λD-$p53^{MLQR}$ phage indicating that this dimeric construct of p53 is folded correctly and, as expected, this interaction was not affected by the addition of up to 384 μM TRTK-12. SBi1 (80 μM), a small molecule that binds S100B [70], was also able to inhibit binding of λD-S100B to λD-$p53^{MLQR}$ (84%) and the binding of λD-S100B to λD-Hdm2 (46%). Together, these competition binding data illustrate that full-length Hdm2 and full-length p53 each bind a site on S100B that comprises the TRTK-12 peptide and the S100B small molecule inhibitor, SBi1 site(s) [64,65,70,71].

3.4. Covalent modifications in the C-terminal negative regulatory domain of p53 protects the tumor suppressor from binding to S100B

It is now established that p53 is protected from Hdm2-dependent degradation via phosphorylation in its N-terminal transactivation domain [72,73]. Based on the 3D structure of S100B bound to the C-terminus of p53, it was predicted that phosphorylated and perhaps acetylated p53 would not bind Ca^{2+}-S100B as tightly as unmodified protein [48]. This indeed turned out to be the case since S100B was found to bind p53 peptides, phosphorylated at residues that were in the S100B–p53 peptide interface (S376, T377), more weakly than a corresponding p53 peptide that was not covalently modified (Fig. 6; Table 1); whereas, phosphorylation of Ser-378, which is facing solution in the S100B–p53 peptide structure had little or no effect on binding (Table 1; Fig 6). Similarly, steric hindrance or loss of a salt bridge due to the acetylation of p53 Lys-383 could explain why the acetylated version of the p53 peptide also inhibits S100B binding by more than 10-fold (Fig. 6A and B). Furthermore, it is likely that covalent modifications such as phosphorylation and perhaps acetylation stabilize the structure of the extreme C-terminus, as predicted by Arrowsmith et al. [49], and as supported by data showing that phosphorylated p53 is more stable and binds DNA more tightly *in vitro* [74].

Further evidence for this "p53 protection model" is provided by our own earlier studies with the Δ30 p53 mutant ($p53^{1–363}$; ΔNRD), which has the C-terminus of p53 removed [25]. In this study, we showed that the Δ30 p53 mutant was down-regulated by S100B to a larger degree than that of full-length p53 in H1299 cells [25]. Here, it is thought that the inability of the Δ30 p53 mutant to get sufficiently phosphorylated leaves this construct open to S100B binding to the tetramer domain, as observed previously ([67]; Table 1), and subsequently to S100B-dependent p53 degradation. Based on this model, we anticipated that the S376A and the T377A p53 mutants (and perhaps others) will be more susceptible to S100B-dependent

Fig. 3. Changes in chemical shifts for $^{1}H–^{15}N$ correlations in Ca^{2+}-bound S100B upon binding several target peptides. Similar residues in S100B undergo chemical shift perturbations upon binding (A) $p53^{367–388}$, (B) $p53^{321–346}$, (C) TRTK-12, (D) $PKC^{19–36}$ or (E) the RKLLW peptides. The bar graphs on the left show the combined backbone ^{1}H and ^{15}N chemical shift perturbations upon peptide binding to Ca^{2+}–S100B except for residues G22, D23, K24, I47, and Q50, which are severely exchanged broadened. Correlations for H42, L44, E45, and E86 for the $p53^{321–346}$ peptide, F43 for TRTK-12, and M79 and V80 for the $PKC^{19–36}$ peptide broadened upon binding, so Δδ values could not be determined for these residues. To the right of each bar graph are ribbon diagrams of the 3D solution structure for $p53^{367–388}$-bound S100B (**PDB 1DT7**) with the $p53^{367–388}$ peptide in each subunit removed; these ribbon diagrams show (in yellow) the amino acid residues having significant chemical shift perturbations (i.e. Δδ values that are greater than that observed for F14) and/or residues for which extreme exchange broadening effects was observed during the peptide titration. The residues that were perturbed (in yellow) are shown for titrations with each peptide, respectively, on only one S100B subunit (red); the other S100B subunit (blue) and the Ca^{2+} ions (gray spheres) are also illustrated.

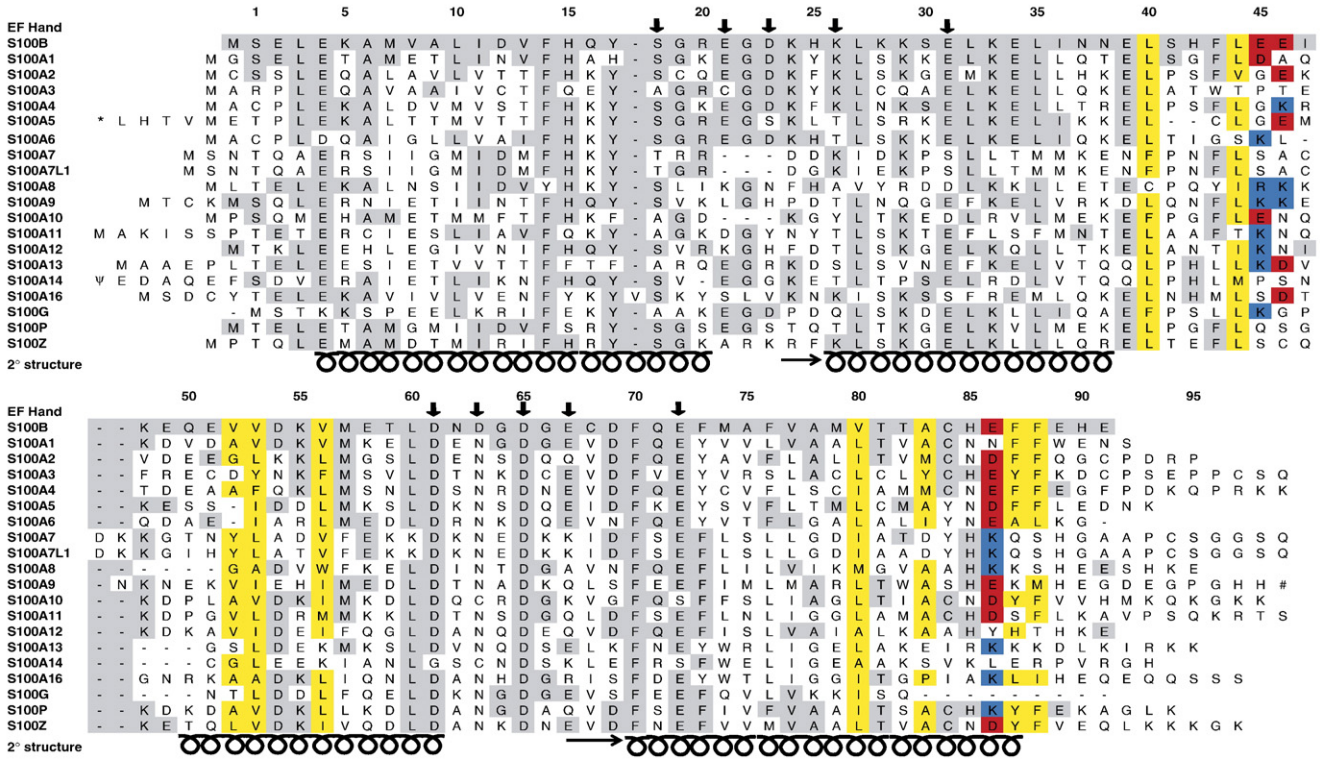

Fig. 4. Sequence alignment of the human S100 protein family based on their homology to S100B. The residues highlighted in gray match the S100B protein sequence exactly; residues highlighted in yellow are conserved hydrophobic residues; residues highlighted in red are conserved negatively charged residues. Shown in blue are a few positively charged residues that appear in regions of the protein that are more often negatively charged to emphasize a change in charge in some S100 family members at that position. In addition, downward pointing arrows are used to identify the position of the Ca^{2+}-binding ligands for both the N-terminal S100-EF-hand (the pseudo EF-hand) and the more typical C-terminal EF-hand. Some S100 proteins are too long for this table, so parts of their sequences are omitted as follows: for S100A5, *=MPAAWILWAHSHSE; for S100A9, #=HKPGLGEGTP; for S100A14, ψ=MGQCRSANA.

degradation than wild-type and S376A p53. In H1299 cells, this indeed turned out to be the case for the T377A mutant (Fig 6C). However, no additional effect on p53 degradation was observed when the T377A p53 and S376A+T377A double mutant were compared, which is evidence that the mutation at Thr-377 is more deleterious for S100B-dependent degradation of p53 in cells, and are consistent with the hypothesis that phosphorylation of Thr-377 in p53 is an important phosphorylation site for protecting p53 from S100B. This idea is also in agreement with cellular reporter gene assays from Youmell et al., done with full-length p53, which show that mutating T377 is the most deleterious PKC site mutant when p53 transcription activation activity is measured; although, a small effect was also observed for the S376 mutant [75]. The differences observed in comparisons of the peptide-binding data (Table 1) to the cellular assays done with full-length p53 (Fig. 6) are suggestive that perhaps full-length p53 binds S100B slightly differently than found in the S100B–p53 peptide complexes, although this remains to be determined more rigorously. Nonetheless, it is important to note that the absence of the extreme C-terminus (Δ30 p53; [25]) and/or the lack of a phosphorylation site in the C-terminus of p53 (at Thr-377) does reduce the stability of p53 in treatments with S100B (Fig. 6C) and is consistent with previously measured transcription activation assays done with the same phosphorylation mutants performed by Youmell et al. [75].

4. Summary

A schematic is presented (Fig. 7) that summarizes how calcium-loaded S100B and Hdm2 participate in the down-regulation of the tumor suppressor protein, p53. Furthermore, feedback loops are in place such that the tumor suppressor protein levels are kept under tight regulatory control (Fig. 7). Evidence of an S100-p53 interaction *in vivo* was provided by co-immunoprecipitation (co-IP) experiments with S100B done in human primary malignant melanoma cancer cells [76]. Similar co-IP experiments were also demonstrated for the S100A4–p53 interaction [24]. While most proteins that bind or modify the C-terminus of p53 activate the tumor suppressor, the opposite effect was observed for both S100A4 and S100B; in both cases, DNA binding to p53 in gel shift assays is decreased, and correspondingly, p53 function as a transcription activator is decreased when bound to S100 protein [24,25]. In the case of S100A4 (mts1), the S100-dependent affect on p53 transcription activation varied for some genes and showed a time and cell-density dependence [24,77]. For S100B, p53 protein levels and downstream effector genes, Hdm2 and p21 were also measured after human large-cell lung carcinoma cells (H1299; p53−/−) were transiently co-transfected with p53 and S100B expression vectors [25,78]. As expected, expression of p53 triggered expression of Mdm2 and p21, but co-expression with the S100B protein markedly reduced the accumulation of p53,

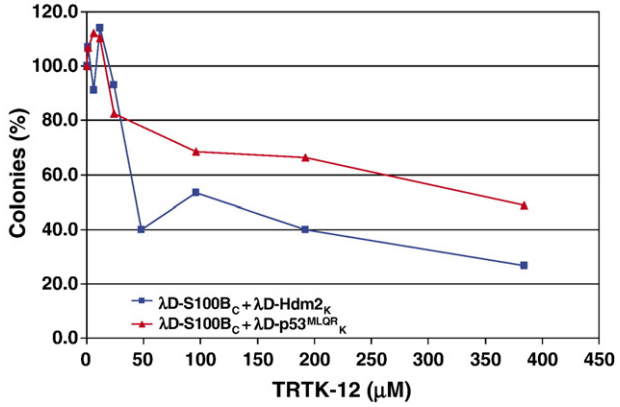

Fig. 5. The p53–S100B, p53–Hdm2, and the Hdm2–S100B interactions are detected using the Lamda2hybrid methodology and then monitored using competition studies with a S100B binding peptide, TRTK-12. Recombinant lambda phage expressing S100B (λD-S100B$_C$) and a mutant of p53 that forms dimer rather than tetramers (λD-p53$^{MLQR}{}_K$) are fused to the C-terminus of the phage major capsid protein D, one containing the Cml^R and the other the Kan^R gene, respectively. Thus, S100B and p53^{MLQR} interact as is necessary to produce double antibiotic resistant colonies (red triangles). This S100B–p53^{MLQR} interaction was inhibited in a dose-dependent manner (red triangles) by the addition of a peptide that binds to S100B specifically, TRTK-12 (Table 1). The same phage expressing S100B was also able to interact with a phage expressing Hdm2 (λD-Hdm2$_K$), and was also inhibited in a dose-dependent manner by TRTK-12 (pink squares).

Hdm2 and p21 protein levels [25]. Similarly, endogenous wild-type p53 in human breast cancer cell line MCF-7 (p53+/+) [79] was inhibited when transiently transfected with S100B [25]. These earlier data indicate that the basal levels of p53, Hdm2 and p21 can be induced by exposure to bleomycin [25], while over-expression of S100B protein reduces p53 levels and its downstream effector genes. Additional evidence that S100B down-regulates p53 protein levels is provided by siRNA data since when S100B levels are reduced using siRNA directed against S100B (siRNA^{S100B}), functional wild-type p53 protein is restored in primary malignant melanoma cells [76].

It is well established that p53 activates the transcription of Hdm2 (Fig. 7), a protein that is involved in ubiquitin-dependent degradation of p53 itself as part of a feedback loop [33,45,80]. In an analogous situation to Hdm2, p53 also activates the transcription of S100 proteins, including S100B [76,81]. The promoter for S100B has six relatively equally spaced sequences that correspond to the consensus sequence for p53 binding (>16/20 nucleotide match), and one region has a nucleotide sequence that matches the p53-binding consensus sequence perfectly (20/20 nucleotide match). In DNA band shift binding assays, regions of the S100B promoter bind p53 and, not surprisingly, the constructs containing the 20/20 matching sequence have the highest DNA binding affinity [25]. Furthermore, p53 activates transcription in reporter gene assays (i.e. CAT assays) containing various constructs of the S100B promoter [76].

It is now clear that the p53-dependent activation of the S100B promoter is also itself negatively regulated. This conclusion was first suspected from a comparison of the transcription activity of the full-length S100B promoter to

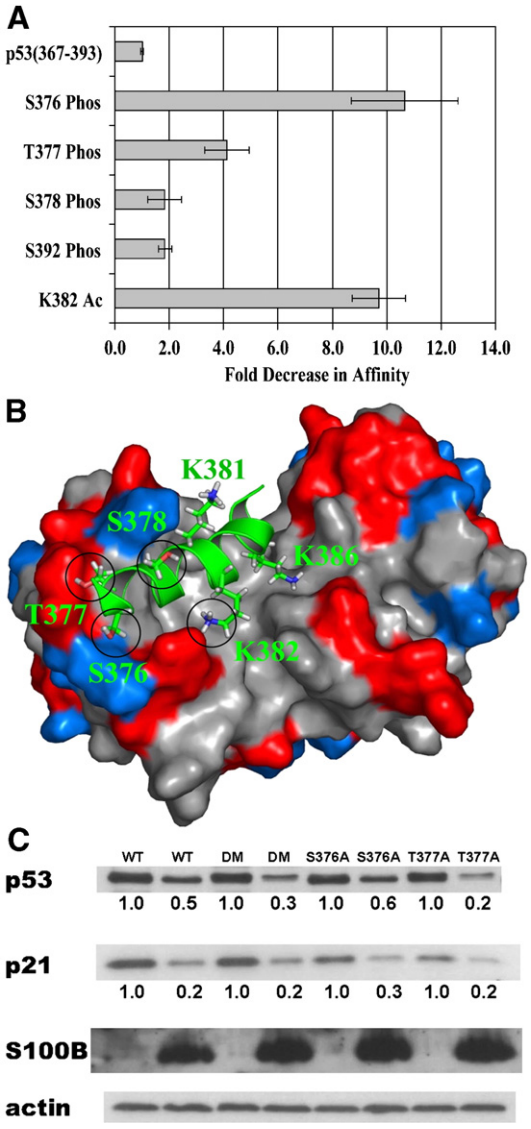

Fig. 6. Phosphorylation and acetylation in the C-terminus of p53 inhibits the S100B–p53 interaction and prevents S100B-dependent down-regulation of the tumor suppressor. These results are analogous to the mechanism for how phosphorylation protects p53 from Hdm2-dependent degradation. (A) The binding of unmodified p53$^{367–393}$ peptide is compared to specifically acetylated (Ac-K382) and phosphorylated (P-S376, P-T377, and P-S378) forms of p53$^{367–393}$. Phosphorylation (at positions S376, T377) and acetylation (at position K382) inhibit the peptide binding to S100B via steric interactions in accordance with the 3D structure of p53$^{367–388}$ peptide bound to Ca^{2+}–S100B (shown in B) [86]. In (C), transient co-transfection of S100B with either wild-type or specific alanine mutations of p53 at Ser-376 (S376A), Thr-377 (T377A) or at both positions (S376A+T377A) are examined in H1299 cells (p53−/−). As observed previously, co-transfections of S100B with wild-type p53 results in a decrease of p53 protein levels and its down-stream gene product, p21, when compared to transient transfections of p53 alone ([25]; lanes 1, 2). However, when a double mutant of p53 (DM; S376A+T377A) is transiently transfected into these same cells (+/−S100B; lanes 3, 4) and compared to similar experiments with the corresponding single mutant proteins (S376A, lanes 5, 6; T377A, lanes 7, 8), it is found that no additional effect is observed with the S376A mutation (versus wild-type p53). These data indicate that the T377A mutation is most deleterious and are consistent data from Youmell et al., who reported that the T377A mutation had the largest effect on p53-dependent transcription activation in cellular assays where these same protein kinase C sites (PKC) were mutated [87] (see text).

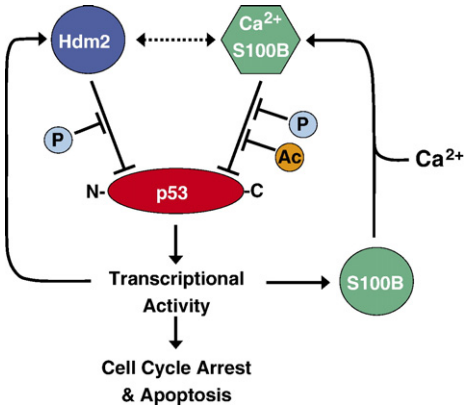

Fig. 7. Scheme illustrating the down-regulation of p53 by the calcium-binding protein S100B and the E3 ubiquitin ligase, Hdm2. In times of cellular stress, covalent modifications (i.e. phosphorylation, blue circled P; acetylation, orange circled Ac) of p53 protect the tumor suppressor from Hdm2- and S100B-dependent binding in the N- and C-terminus of p53 (red oval) respectively, and subsequent down-regulation of p53 protein levels. The interaction of S100B with p53 requires that S100B binds calcium and undergoes a conformational change (green circle→green hexagon). When p53 protein levels increase, feedback control is in place since transcription of the S100B and Hdm2 genes are both activated by elevated levels of p53 [76]. An interaction between S100B and Hdm2 was also detected as described here (Table 1; (Figs. 1, 2, 5)); however, the cellular and mechanistic consequences of this interaction require further investigation, so this newly discovered protein–protein interaction is represented by a dotted two-headed arrow.

promoter constructs from a gene involved in cell-cycle control such as GADD45 [76]. While none of the GADD45 sites have a 20/20 matching sequence, this promoter is more highly activated by p53 than the S100B promoter. Furthermore, removing portions of the S100B promoter increases its p53-dependent transcription activation, which is consistent with the S100B promoter being negatively regulated when the full-length promoter is intact. However, if the 20/20 p53 consensus region of the S100B promoter is removed, then, not surprisingly, the p53-dependent transcription activation activity was diminished significantly [76]. Negative regulation of the p53 region of the S100B promoter is logical because genes involved in p53 function ought to be activated prior to genes such as S100B and Hdm2, which ultimately negatively regulate p53. In summary, like other proteins such as Pirh2 [82], COP1 [83] and Hdm2 that down regulate p53, S100B is also (i) activated at the transcriptional level by p53 and (ii) then subsequently inhibits p53 function via feedback control. The important distinction between S100B and these other proteins is that the S100B interaction with the C-terminus of p53 is Ca^{2+}-dependent and links p53 biology to extracellular growth responses; whereas, Hdm2, COP1, and Pirh2 all interact more towards the N-terminus of p53 than S100B and do not depend on calcium for binding the tumor suppressor [61].

Overall, p53 is activated upon DNA damage or under stress and up regulates the transcription of genes involved in apoptosis (i.e. ↑Bax etc.) and cell cycle-dependent growth arrest (i.e. ↑p21 etc.) (Fig. 7). Under such conditions, it is now thought that p53 is protected from Hdm2 and S100B by covalent modification in its transactivation domain and in its extreme C-terminus, respectively (Figs. 6, 7). As part of a feedback control mechanism, p53 also up regulates the transcription of genes involved in its own inactivation (i.e. Hdm2 and S100B). In a cell growth response, there is an increase in intracellular calcium (↑Ca^{2+}), and S100B binds calcium and undergoes a conformational change as is necessary to interact with the tumor suppressor protein, p53. This Ca^{2+}-dependent interaction between S100B and p53 induces a conformational change in p53 and tetramer dissociation of the tumor suppressor [66], which likely contributes to its degradation (i.e. perhaps involving Hdm2/ubiquitin-and/or protease-dependent pathways). Thus, down-regulation of p53 by S100B and Hdm2 ultimately facilitates cell growth. The newly discovered interaction described here between S100B and Hdm2 further implies that these two proteins may work together to down-regulate p53; however, the relevance of this interaction needs to be explored in more detail in vivo. This interaction between S100B and the E3 ligase for p53 ubiquitination, Hdm2, is particularly intriguing because of precedence for an S100 protein, S100A6, interacting with an E3 ubiquitin ligase, now called CacyBP/SIP; this E3 ubiquitin ligase, in turn, interacts with Siah-1 and Skp1 and contributes to the ubiquitination and degradation of beta-catenin [84,85].

The therapeutic relevance of inhibiting S100B is now established because (i) S100B contributes to the depletion of wild-type p53 protein in malignant melanoma and (ii) because S100B protein levels are elevated in this and other cancers. Therefore, such an effort to restore wild-type p53 tumor suppressor function, as is typically found in melanoma, is now underway using a rational drug design approach to find small molecule inhibitors of S100B [70] that mimic, in some respects, the activities observed previously with siRNA directed against S100B [76]. The next step in this process is to fully understand the target-binding site on S100B and how this site is different from other S100 proteins. In this paper, the p53 binding site on S100B is explored in detail, so that inhibitors can more readily be prepared that bind S100B specifically. Furthermore, these studies led to the discovery of a new and likely an important protein–protein interaction between S100B and Hdm2 and possibly with another regulator of p53, Hdm4. Lastly, data were presented that show how cells may prevent the S100B–p53 interaction, via phosphorylation and acetylation. These data suggest that the mechanism for the protection of the p53 tumor suppressor from two of its known negative-regulatory proteins, S100B and Hdm2, *in vivo*, is likely to be a very similar one (i.e. via covalent modification of the tumor suppressor).

Acknowledgments

We would like to thank Nathan Wright for useful discussions with regard to the target binding site of several S100 proteins.

These studies were supported by grants from the National Institutes of Health (GM58888; CA107331 to DJW) and from the American Cancer Society (CDD 107745 to DJW). The NMR spectrometers used in these studies were purchased, in part, with funds from shared instrumentation grants from the NIH (S10 RR10441; S10 RR15741; S10 RR16812 to DJW) and from the NSF (DBI 0115795 to DJW). The research was

partially supported by Intramural Research at NIH, NCI, Center for Cancer Research (to ABO and SA).

References

[1] D.B. Zimmer, E.H. Cornwall, A. Landar, W. Song, The S100 protein family: history, function, and expression, Brain Res. Bull. 37 (1995) 417–429.

[2] R. Donato, S100: a multigenic family of calcium-modulated proteins of the EF-hand type with intracellular and extracellular functional roles, Int. J. Biochem. Cell Biol. 33 (2001) 637–668.

[3] C.W. Heizmann, The multifunctional S100 protein family, Methods Mol. Biol. 172 (2002) 69–80.

[4] B. Moore, A soluble protein characteristic of the nervous system, Biochem. Biophys. Res. Comm. 19 (1965) 739–744.

[5] F. Castets, W.S. Griffin, A. Marks, L.J. Van Eldik, Transcriptional regulation of the human S100 beta gene, Brain Res. 46 (1997) 208–216.

[6] L.J. Van Eldik, W.S.T. Griffen, S100b expression in Alzheimer's disease: relation to neuropathology in brain regions, Biochimica et Biophysica Acta 1223 (1994) 398–403.

[7] M.A. Mariggio, S. Fulle, P. Calissano, I. Nicoletti, G. Fano, The brain protein S-100ab induces apoptosis in PC12 cells, Neuroscience 60 (1994) 29–35.

[8] R.E. McLendon, W.W. Vick, S.H. Bigner, D.D. Bigner, Monoclonal antibodies and diagnosis of brain neoplasms, in: H.Z. Kubchik (Ed.), Cancer Diagnosis in vitro Using Monoclonal Antibodies, Marcel Dekker, New York, 1988, pp. 31–66.

[9] L.O. Hansson, E. Vonschoultz, E. Djureen, J. Hansson, B. Nilsson, U. Ringborg, Prognastic value of serum analyses of S100 protein beta in malignant melanoma, Anticancer Res. 17 (1997) 3071–3073.

[10] K. Stoitchkov, S. Letellier, J.P. Garnier, B. Bousquet, N. Tsankov, P. Morel, G. Ghanem, T. Le Bricon, Melanoma progression and serum L-dopa/L-tyrosine ratio: a comparison with S100B, Melanoma Res. 12 (2002) 255–262.

[11] M.Q. Mohammed, H.D. Abraha, R.A. Sherwood, K. MacRae, S. Retsas, Serum S100beta protein as a marker of disease activity in patients with malignant melanoma, Med. Oncol. 18 (2001) 109–120.

[12] G. Ghanem, B. Loir, R. Morandini, F. Sales, D. Lienard, A. Eggermont, F. Lejeune, E.M.G. The, On the release and half-life of S100B protein in the peripheral blood of melanoma patients, Int. J. Cancer 94 (2001) 586–590.

[13] M. Takashi, T. Sakata, Y. Nakano, Y. Yamada, K. Miyake, K. Kato, Elevated concentrations of the beta-subunit of S100 protein in renal cell tumors in rats, Urol. Res. 22 (1994) 251–255.

[14] H. Suzushima, N. Asou, T. Hattori, K. Takatsuki, Adult T-cell leukemia derived from S100-beta positive double-negative (CD4-CD8-) T cells, Leuk. Lymphoma 13 (1994) 257–262.

[15] D.A. Hinkle, J.P. Harney, A. Cai, D.C. Hilt, P.J. Yarowsky, P.M. Wise, Basic fibroblast growth factor-2 and interleukin-1-Beta regulate S100-beta expression in cultured astrocytes, Neuroscience 82 (1998) 33–41.

[16] D. Kligman, D. Hilt, The S100 protein family, Trends Biochem. Sci. 13 (1988) 437–443.

[17] M. Pedrocchi, B.W. Schafer, H. Mueller, U. Eppenberger, C.W. Heizmann, Expression of Ca^{2+}-binding proteins of the S100 family in malignant human breast-cancer cell lines and biopsy samples, Int. J. Cancer 57 (1994) 684–690.

[18] D. Chen, M.P. Davies, P.S. Rudl, R. Barraclough, Transcriptional down-regulation of the metastasis-inducing S100A4 (p9Ka) in benign but not in malignant rat mammary epithelial cells by GC-factor, J. Biol. Chem. 272 (1997) 20283–20290.

[19] K. Takenaga, Y. Nakamura, S. Sakiyama, Expression of antisense RNA to S100A4 gene encoding an S100-related calcium-binding protein suppresses metastatic potential of high-metastatic Lewis lung carcinoma cells, Oncogene 14 (1997) 331–337.

[20] G.M. Maelandsmo, V.A. Florenes, T. Mellingsaeter, E. Hovig, R.S. Kerbel, O. Fodstad, Differential expression patterns of S100A2, S100A4 and S100A6 during progression of human malignant melanoma, Int. J. Cancer 74 (1997) 464–469.

[21] R. Boni, G. Burg, A. Doguoglu, E.C. Ilg, B.W. Schafer, B. Muller, C.W. Heizmann, Immunohistochemical localization of the Ca^{2+} binding S100 proteins in normal human skin and melanocytic lesions, Br. J. Dermatol. 137 (1997) 39–43.

[22] X.Q. Xia, S.W. Stoll, M. Liebert, S.P. Ethier, T. Carey, R. Esclamado, W. Carroll, T.M. Johnson, J.T. Elder, CAN19 expression in benign and malignant hyperplasias of the skin and oral mucosa—Evidence for a role in regenerative differentiation, Cancer Res. 57 (1997) 3055–3062.

[23] L.O. Hansson, E. von Schoultz, E. Djureen, J. Hansson, B. Nilsson, U. Ringborg, Prognostic value of serum analyses of S-100 protein beta in malignant melanoma, Anticancer Res. 17 (1997) 3071–3073.

[24] M. Grigorian, S. Andresen, E. Tulchinsky, M. Kriajevska, C. Carlberg, C. Kruse, M. Cohn, N. Ambartsumian, A. Christensen, G. Selivanova, E. Lukanidin, Tumor suppressor p53 protein is a new target for the metastasis-associated Mts1/S100A4 protein: functional consequences of their interaction, J. Biol. Chem. 276 (2001) 22699–22708.

[25] J. Lin, M. Blake, C. Tang, D. Zimmer, R.R. Rustandi, D.J. Weber, F. Carrier, Inhibition of p53 transcriptional activity by the S100B calcium-binding protein, J. Biol. Chem. 276 (2001) 35037–35041.

[26] F. Carrier, M. Blake, D. Zimmer, R.R. Rustandi, D.J. Weber, Abrogation of p53 transcriptional activity by the S100 calcium binding proteins: Possible implication in angiogenesis, Proc. AACR 40 (1999) 102.

[27] A.J. Levine, J. Mom, C.A. Finlay, The p53 tumour suppressor gene, Nature 351 (1991) 453–456.

[28] A.J. Levine, p53, the cellular gatekeeper for growth and division, Cell 88 (1997) 323–331.

[29] D.B. Woods, K.H. Vousden, Regulation of p53 function, Exp. Cell Res. 264 (2001) 56–66.

[30] T.F. Burns, W.S. El-Deiry, The p53 pathway and apoptosis, J. Cell. Physiol. 181 (1999) 231–239.

[31] E. Appella, C.W. Anderson, Post-translational modifications and activation of p53 by genotoxic stresses, Eur. J. Biochem. 268 (2001) 2764–2772.

[32] C.H. Arrowsmith, Structure and function in the p53 family, Cell Death Differ. 6 (1999) 1169–1173.

[33] C. Prives, P.A. Hall, The p53 pathway, J. Pathol. 187 (1999) 112–126.

[34] K.H. Vousden, p53: death star, Cell 103 (2000) 691–694.

[35] K.M. Ryan, A.C. Phillips, K.H. Vousden, Regulation and function of the p53 tumor suppressor protein, Curr. Opin. Cell Biol. 13 (2001) 332–337.

[36] M.L. Agarwal, W.R. Taylor, M.V. Chernov, O.B. Chernova, G.R. Stark, The p53 network, J. Biol. Chem. 273 (1998) 1–4.

[37] S.D. Tyner, S. Venkatachalam, J. Choi, S. Jones, N. Ghebranious, H. Igelmann, X. Lu, G. Soron, B. Cooper, C. Brayton, S. Hee Park, T. Thompson, G. Karsenty, A. Bradley, L.A. Donehower, p53 mutant mice that display early ageing-associated phenotypes, Nature 415 (2002) 45–53.

[38] T. Minamoto, T. Buschmann, H. Habelhah, E. Matusevich, H. Tahara, A.L. Boerresen-Dale, C. Harris, D. Sidransky, Z. Ronai, Distinct pattern of p53 phosphorylation in human tumors, Oncogene 20 (2001) 3341–3347.

[39] L. Jayaraman, C. Prives, Covalent and noncovalent modifiers of the p53 protein, Cell Mol. Life. Sci. 55 (1999) 76–87.

[40] G.S. Jimenez, S.H. Khan, J.M. Stommel, G.M. Wahl, p53 regulation by post-translational modification and nuclear retention in response to diverse stresses, Oncogene 18 (1999) 7656–7665.

[41] D.W. Meek, Post-translational modifications of p53 and the integration of stress signals, Pathol. Biol. 45 (1997) 804–814.

[42] P.D. Jeffrey, S. Gorina, N.P. Pavletich, Crystal stucture of the tetramerization domain of the p53 tumor suppressor at 1.7 Angstroms, Science 267 (1995) 1498–1502.

[43] W. Lee, T.S. Harvey, Y. Yin, P. Yau, D. Litchfield, C.H. Arrowsmith, Solution structure of the tetrameric minimum transforming domain of p53, Nat. Struct. Biol. 1 (1994) 877–890.

[44] G.M. Clore, J.G. Omichinski, K. Sakaguchi, N. Zambrano, H. Sakamoto, E. Appella, A.M. Gronenborn, High-resolution structure of the oligomerization domain of p53 by multidimensional NMR, Science 265 (1994) 386–391.

[45] D.A. Freedman, L. Wu, A.J. Levine, Functions of the MDM2 oncoprotein, Cell Mol. Life Sci. 55 (1999) 96–107.

[46] E.J. Milner-White, The N-terminal domain of Mdm2 resembles calmodulin and its relatives, J. Mol. Biol. 286 (1999) 957–963.
[47] J.C. Marine, A.G. Jochemsen, Mdmx as an essential regulator of p53 activity, Biochem. Biophys. Res. Commun. 331 (2005) 750–760.
[48] R.R. Rustandi, D.M. Baldisseri, D.J. Weber, Structure of the negative regulatory domain of p53 bound to S100B, Nat. Struct. Biol. 7 (2000) 570–574.
[49] A. Ayed, F.A. Mulder, G.S. Yi, Y. Lu, L.E. Kay, C.H. Arrowsmith, Latent and active p53 are identical in conformation, Nat. Struct. Biol. 8 (2001) 756–760.
[50] D.P. Lane, Cancer. p53, guardian of the genome, Nature 358 (1992) 15–16.
[51] A.C. Drohat, D.M. Baldisseri, R.R. Rustandi, D.J. Weber, Solution structure of calcium-bound rat S100B as determined by nuclear magnetic resonance spectroscopy, Biochemistry 37 (1998) 2729–2740.
[52] N.T. Wright, K.M. Varney, K.C. Ellis, J. Markowitz, R.K. Gitti, D.B. Zimmer, D.J. Weber, The three-dimensional solution structure of Ca(2+)-bound S100A1 as determined by NMR spectroscopy, J. Mol. Biol. 353 (2005) 410–426.
[53] Y. Cheng, W.H. Prusoff, Relationship between the inhibition constant (K1) and the concentration of inhibitor which causes 50 per cent inhibition (I50) of an enzymatic reaction, Biochem. Pharmacol. 22 (1973) 3099–3108.
[54] Z. Nikolovska-Coleska, R. Wang, X. Fang, H. Pan, Y. Tomita, P. Li, P.P. Roller, K. Krajewski, N.G. Saito, J.A. Stuckey, S. Wang, Development and optimization of a binding assay for the XIAP BIR3 domain using fluorescence polarization, Anal. Biochem. 332 (2004) 261–273.
[55] P.T. Wilder, D.M. Baldisseri, R. Udan, K.M. Vallely, D.J. Weber, Location of the Zn(2+)-binding site on S100B as determined by NMR spectroscopy and site-directed mutagenesis, Biochemistry 42 (2003) 13410–13421.
[56] A.S. Edison, F. Abildgaard, W.M. Westler, E.S. Mooberry, J.L. Markley, Practical introduction to theory and implementation of multinuclear, multidimensional nuclear magnetic resonance experiments, Methods Enzymol. 239 (1994) 3–79.
[57] D.H. Live, D.G. Davis, W.C. Agosta, D. Cowburn, J. Am. Chem. Soc. (1984) 1939–1941.
[58] S. Spera, M. Ikura, A. Bax, Measurement of the exchange rates of rapidly exchanging amide protons: application to the study of calmodulin and its complex with a myosin light chain kinase fragment, J. Biomol. NMR 1 (1991) 155–165.
[59] S. Mori, C. Abeygunawardana, M.O. Johnson, P.C. van Zijl, Improved sensitivity of HSQC spectra of exchanging protons at short interscan delays using a new fast HSQC (FHSQC) detection scheme that avoids water saturation, J. Magn. Reson. B 108 (1995) 94–98.
[60] T.S. Davison, X. Nie, W. Ma, Y. Lin, C. Kay, S. Benchimol, C.H. Arrowsmith, Structure and functionality of a designed p53 dimer, J. Mol. Biol. 307 (2001) 605–617.
[61] D.J. Weber, R.R. Rustandi, F. Carrier, D.B. Zimmer, Interaction of Dimeric S100B(bb) with the Tumor Suppressor Protein: A Model for Ca-Dependent S100-Target Protein Interactions, Kluwer Academic Publishers, Dordrecht, The Netherlands, 2000.
[62] V.V. Ivanenkov, G.A. Jamieson Jr., E. Gruenstein, R.V. Dimlich, Characterization of S-100b binding epitopes. Identification of a novel target, the actin capping protein, CapZ, J. Biol. Chem. 270 (1995) 14651–14658.
[63] S. Bhattacharya, E. Large, C.W. Heizmann, B. Hemmings, W.J. Chazin, Structure of the Ca^{2+}/S100B/NDR kinase peptide complex: insights into S100 target specificity and activation of the kinase, Biochemistry 42 (2003) 14416–144126.
[64] K.G. Inman, R. Yang, R.R. Rustandi, K.E. Miller, D.M. Baldisseri, D.J. Weber, Solution NMR structure of S100B bound to the high-affinity target peptide TRTK-12, J. Mol. Biol. 324 (2002) 1003–1014.
[65] K.A. McClintock, G.S. Shaw, A novel S100 target conformation is revealed by the solution structure of the Ca^{2+}–S100B–TRTK-12 complex, J. Biol. Chem. 278 (2003) 6251–6257.
[66] J. Baudier, C. Delphin, D. Grunwald, S. Khochbin, J.J. Lawrence, Characterization of the tumor suppressor protein p53 as a protein kinase C substrate and a S100b-binding protein, Proc. Natl. Acad. Sci. U. S. A. 89 (1992) 11627–11631.
[67] M.R. Fernandez-Fernandez, D.B. Veprintsev, A.R. Fersht, Proteins of the S100 family regulate the oligomerization of p53 tumor suppressor, Proc. Natl. Acad. Sci. U. S. A. 102 (2005) 4735–4740.
[68] R.R. Rustandi, D.M. Baldisseri, A.C. Drohat, D.J. Weber, Structural changes in the C-terminus of Ca^{2+}-bound rat S100B (beta beta) upon binding to a peptide derived from the C-terminal regulatory domain of p53, Protein Sci. 8 (1999) 1743–1751.
[69] R.R. Rustandi, A.C. Drohat, D.M. Baldisseri, P.T. Wilder, D.J. Weber, The Ca^{2+}-dependent interaction of S100B with a peptide derived from p53, Biochemistry 37 (1998) 1951–1960.
[70] J. Markowitz, I. Chen, R. Gitti, D.M. Baldisseri, Y. Pan, R. Udan, F. Carrier, A.D. MacKerell Jr., D.J. Weber, Identification and characterization of small molecule inhibitors of the calcium-dependent S100B–p53 tumor suppressor interaction, J. Med. Chem. 47 (2004) 5085–5093.
[71] J. Markowitz, A.D. MacKerell Jr., F. Carrier, T.H. Charpentier, D.J. Weber, Design of inhibitors for S100B, Curr. Top. Med. Chem. 5 (2005) 1093–1108.
[72] T. Iwakuma, G. Lozano, MDM2, an introduction, Mol. Cancer Res. 1 (2003) 993–1000.
[73] O. Schon, A. Friedler, M. Bycroft, S.M. Freund, A.R. Fersht, Molecular mechanism of the interaction between MDM2 and p53, J. Mol. Biol. 323 (2002) 491–501.
[74] D.P. Lane, C.A. Midgley, T.R. Hupp, X. Lu, B. Vojtesek, S.M. Picksley, On the regulation of the p53 tumour suppressor, and its role in the cellular response to DNA damage, Philos. Trans. R. Soc. Lond., B Biol. Sci. 347 (1995) 83–87.
[75] M. Youmell, S.J. Park, S. Basu, B.D. Price, Regulation of the p53 protein by protein kinase C and protein kinase z, Biochem. Biophys. Res. Commun. 245 (1998) 514–518.
[76] J. Lin, Q. Yang, Z. Yan, J. Markowitz, P.T. Wilder, F. Carrier, D.J. Weber, Inhibiting S100B restores p53 levels in primary malignant melanoma cancer cells, J. Biol. Chem. 279 (2004) 34071–34077.
[77] S.C. Garrett, K.M. Varney, D.J. Weber, A.R. Bresnick, S100A4: a mediator of metastasis, J. Biol. Chem. 281 (2006) 677–680.
[78] W.D. Funk, D.T. Pak, R.H. Karas, W.E. Wright, J.W. Shay, A transcriptionally active DNA-binding site for human p53 protein complexes, Mol. Cell Biol. 12 (1992) 2866–2871.
[79] M.B. Kastan, Q. Zhan, W.S. el-Deiry, F. Carrier, T. Jacks, W.V. Walsh, B.S. Plunkett, B. Vogelstein, A.J. Fornace Jr., A mammalian cell cycle checkpoint pathway utilizing p53 and GADD45 is defective in ataxia–telangiectasia, Cell 71 (1992) 587–597.
[80] J. Momand, H.H. Wu, G. Dasgupta, MDM2—Master regulator of the p53 tumor suppressor protein, Gene 242 (2000) 15–29.
[81] M. Tan, C.W. Heizmann, K. Guan, B.W. Schafer, Y. Sun, Transcriptional activation of the human S100A2 promoter by wild-type p53, FEBS Lett. 445 (1999) 265–268.
[82] R.P. Leng, Y. Lin, W. Ma, H. Wu, B. Lemmers, S. Chung, J.M. Parant, G. Lozano, R. Hakem, S. Benchimol, Pirh2, a p53-induced ubiquitin-protein ligase, promotes p53 degradation, Cell 112 (2003) 779–791.
[83] D. Dornan, I. Wertz, H. Shimizu, D. Arnott, G.D. Frantz, P. Dowd, K. O'Rourke, H. Koeppen, V.M. Dixit, The ubiquitin ligase COP1 is a critical negative regulator of p53, Nature 429 (2004) 86–92.
[84] A. Filipek, S100A6 and CacyBP/SIP—Two proteins discovered in Ehrlich Ascites tumor cells that are potentially involved in the degradation of beta-catenin, Chemotherapy 52 (2005) 32–34.
[85] A. Filipek, B. Jastrzebska, M. Nowotny, J. Kuznicki, CacyBP/SIP, a calcyclin and Siah-1-interacting protein, binds EF-hand proteins of the S100 family, J. Biol. Chem. 277 (2002) 28848–28852.
[86] R.R. Rustandi, D.M. Baldisseri, D.J. Weber, Structure of the negative regulatory domain of p53 bound to S100B(betabeta), Nat. Struct. Biol. 7 (2000) 570–574.
[87] M. Youmell, S.J. Park, S. Basu, B.D. Price, Regulation of the p53 protein by protein kinase Ca and protein kinase Cz, Biochem. Biophys. Res. Commun. 245 (1998) 514–518.
[88] K.G. Inman, R. Yang, R.R. Rustandi, K.E. Miller, D.M. Baldisseri, D.J. Weber, Solution NMR structure of S100B bound to the high-affinity target peptide TRTK-12, J. Mol. Biol. 324 (2002) 1003–1014.
[89] K.A. McClintock, L.J. Van Eldik, G.S. Shaw, The C-terminus and linker region of S100B exert dual control on protein–protein interactions with TRTK-12, Biochemistry 41 (2002) 5421–5428.

[90] M.R. Fernandez-Fernandez, D.B. Veprintsev, A.R. Fersht, Proteins of the S100 family regulate the oligomerization of p53 tumor suppressor, Proc. Natl. Acad. Sci. U. S. A. 102 (2005) 4735–4740.
[91] T. Duda, K.W. Koch, V. Venkataraman, C. Lange, M. Beyermann, R.K. Sharma, Ca(2+) sensor S100beta-modulated sites of membrane guanylate cyclase in the photoreceptor-bipolar synapse, EMBO J. 21 (2002) 2547–2556.
[92] C. Delphin, M. Ronjat, J.C. Deloulme, G. Garin, L. Debussche, Y. Higashimoto, K. Sakaguchi, J. Baudier, Calcium-dependent interaction of S100B with the C-terminal domain of the tumor suppressor p53, J. Biol. Chem. 274 (1999) 10539–10544.
[93] P.T. Wilder, D.J. Weber, S100B inhibition of PKC alpha and PKM phosphorylation of a synthetic peptide derived from p53. Biophys. J. 70 (1996) A62.
[94] F.S. Sheu, F.L. Huang, K.P. Huang, Differential responses of protein kinase C substrates (MARCKS, neuromodulin, and neurogranin) phosphorylation to calmodulin and S100, Arch. Biochem. Biophys. 316 (1995) 335–342.
[95] J. Baudier, D. Mochly-Rosen, A. Newton, S.H. Lee, D.E. Koshland Jr., R.D. Cole, Comparison of S100b protein with calmodulin: interactions with melittin and microtubule-associated tau proteins and inhibition of phosphorylation of tau proteins by protein kinase C, Biochemistry 26 (1987) 2886–2893.